Polymer Bulletin
https://doi.org/10.1007/s00289-019-02731-0

ORIGINAL PAPER

Influence of wood surface chemistry on the tensile and flexural properties of heat-treated mangrove/high-density polyethylene composites

Ganiyat Olusola Adebayo[1,2] · Aziz Hassan[1] · Rosiyah Yahya[1] · Normasmira Abd Rahman[1] · Ruth Lafia-Araga[3]

Received: 28 September 2018 / Revised: 22 February 2019 / Accepted: 25 February 2019
© Springer-Verlag GmbH Germany, part of Springer Nature 2019

Abstract

Mangrove wood fiber (MF) was treated at four different temperatures (120 °C, 140 °C, 160 °C and 180 °C) in order to improve its compatibility with polymer matrix. The chemo-structural, thermal and morphological characteristics of untreated and treated MF were analyzed. The chemical composition of the treated MF showed an increase in cellulose content from 46 to 56% at 120 °C, which decreased at further heating. The non-cellulosic constituents of the fiber were removed as indicated by the reduction in magnitude of absorbance peaks mainly at 3343 cm^{-1} and 1027 cm^{-1} in Fourier transform infrared spectroscopy. The X-ray diffraction depicted increased crystallinity with increased temperature due to the conversion of amorphous cellulose and some hemicelluloses to crystalline structures. Color spectroscopy showed higher values of lightness (L^*) at 120 °C and 140 °C, with a corresponding increase in chroma coordinate a^* and decrease in b^* due to the chemical changes that occurred during the heat treatment. Surface morphology by field emission scanning electron microscopy revealed that heat treatment exposed the inner fibrillar feature of fiber, thereby increasing the roughness of the fiber surface. Thermogravimetry analysis further indicated that heat-treated MFs are more stable. Heat treatment improved the tensile strength and modulus of composites as fiber loading increased, while the flexural strength and modulus also showed the same trend. SEM images of tensile fractured surface indicated that the interfacial interaction between the matrix and untreated MF is weaker than the heat-treated specimens.

Keywords Mangrove wood · Thermal analysis · Surface treatments · Mechanical properties · Wood polymer composites · Cellulose

✉ Ganiyat Olusola Adebayo
adebayoganiyat44@gmail.com

✉ Aziz Hassan
ahassan@um.edu.my

Extended author information available on the last page of the article

Published online: 01 March 2019

Introduction

As a result of the increase in environmental awareness, exhaustion of petroleum resources and health-related challenges, the past few years have witnessed a tremendous shift toward the development of new materials derived from biorenewable sources. Nowadays, natural fibers [1–3] are fast evolving as potential substitutes to inorganic/synthetic materials for various applications as building materials and automotive components. There is also a dare need to replace petroleum-based materials with environmentally friendly and sustainable resources. Recently, modifications of thermoplastics by cellulose-based fillers are creating considerable interest especially due to more favorable processing effect (being non-abrasive when compared to mineral-filled materials) [4]. In addition, natural fibers pose some economic advantages when compared to synthetic/inorganic fibers as a result of their abundance, biodegradability, recyclability and lower cost. These advantages make them relevant and widely accepted by automobile, textile and construction industries [5–7]. The exceptional mechanical and physical properties exhibited by lignocellulose fibers, combined with their low density, make this new form of fiber an excellent material for composite reinforcement. Hydrophilic natural fibers have the limitation of incompatibility with a hydrophobic plastic matrix. Hence, there is poor adhesion and inability to transfer stress from the matrix to the fiber, thereby reducing the mechanical strength and ductility. In view of this shortcoming, it is important that natural fibers are subjected to surface modification to enhance the compatibility and adhesion between fibers and matrices. Chemical surface treatments including alkali, silane, acetyl, benzyl, acryl, permanganate, peroxide and isocyanate had been reported [8, 9]. The accompanied by-products of these chemical treatments posed some threats to the environment. On the other hand, physical treatments of natural fibers such as heat and plasma are environmentally friendly, as they do not discharge any by-product.

During heat treatment of wood, the cell wall components in all mass of the wood sample are modified. This enhances durability, increases dimensional stability and reduces shrinkage and swelling due to moisture absorption [10]. Heat modification of wood fiber has an affirmative outcome on its strength properties since the wood's hydrophilicity is lowered and the maximum amount of water is reduced. Increased amount of bound water reduces the hydrogen bonding within the organic polymers of the cell wall, thereby reducing the strength of wood, which is related to covalent and hydrogen intrapolymer bonds [11, 12]. It has been reported that at temperatures above 150 °C, the physical and chemical properties of wood fiber are permanently changed and the strength properties start to weaken [13]. Chemical composition, physical (color), thermal properties and morphological structure of the fiber can be measured to figure out their capability to be utilized as a reinforcing material/filler in biocomposite applications [14].

Mangroves are hard woody plants dominating the coastal areas of tropical and subtropical regions. Mangroves covered approximately 60–75% of the world's tropical and subtropical coastlines [8]. Malaysia has about 645,852 hectares of mangroves, the third largest in the Asia pacific region, and Peninsular Malaysia

has one of the most diverse mangrove assemblages in the world, with at least 38 exclusive and 57 non-exclusive and associate mangrove species. Mangroves have evolved a suite of adaptations to cope with extreme environmental conditions that include high salinity, strong winds, tidal variations, high temperature and anaerobic tidal swamps [15]. In recent years, the ecological, environmental and socioeconomic importance of mangroves have been emphasized by international agencies, governments, local authorities, non-government organizations (NGOs), coastal communities and scientists [16]. To the author's knowledge, research on the utilization of thermally treated mangrove fiber (MF) as a reinforcement material in polymer composite is rather rare.

Furthermore, high-density polyethylene (HDPE) is one of the most widely used plastic materials. The highly crystalline nature of HDPE is responsible for its higher density and stiffness, as well as its low permeability and high chemical resistance. Previous researches have indicated that the addition of natural fibers, such as jute, flax, mica and sisal fibers, into HDPE matrix resulted improved impact, tensile and flexural strengths of HDPE [7, 16]. Generally, high fiber content produced materials with high rigidity. In the study of wood sawdust/high-density polyethylene (HDPE) composites by Bouafif et al., it was observed that the tensile modulus of elasticity (MOE) of composites increased steadily with wood fiber content from 0.85 GPa for neat HDPE to 1.75 GPa for the resultant composites with 45% wood content [17]. Lafia-Araga et al. also reported an enhancement in tensile modulus, flexural strength, flexural modulus and a decrease in tensile strength, as wood content increased in heat-treated Red Balau wood sawdust/low-density polyethylene (LDPE) composites [18]. Owing to the excellent processing properties of HDPE and the relative abundance of MF, combining thermally modified MF with HDPE, will lead to a new product which combines the strength of wood with the ease of processing and aesthetic characteristics of plastics. This will offer a unique and durable product that extends the applications of HDPE beyond its normal usage because of the improved properties conferred by the wood. Therefore, in this study, fibers from mangrove stem were thermally modified at four different temperatures and different techniques were used to characterize the lignocellulosic fibers in order to determine the chemical composition, chemical structure, morphology, crystallinity index and thermal stability. Further, the consequence of thermal modification on tensile and flexural properties of mangrove fiber-reinforced HDPE were examined. This study is aimed at determining the optimal treatment temperature of lignocellulosic mangrove fiber and to explore the reinforcing potential of utilizing heat-modified MF in wood thermoplastic composites (WTCs) via tensile and flexural characterizations.

Materials and methods

Materials

The stem of mangrove wood, Rhizophora stylosa (spotted mangrove), used as raw material was obtained from Matang mangrove Eco-Educational Centre, Perak, Malaysia. The raw wood was processed by chipping and crushing into wood

particle at Fiber and Biocomposite Centre (FIDEC) of the Malaysian Timber Industries Board (MTIB), Banting, Selangor, Malaysia.

Preparation of mangrove fiber

The mangrove particle was sieved to obtain an average particle size of 0.75 mm (mesh size 27) and dried in a vacuum oven at 80 °C for 24 h to a constant weight in order to reduce the moisture content in the fiber. The vacuum-dried fiber was later treated at four different temperatures of 120 °C, 140 °C, 160 °C and 180 °C in an oven under anoxic condition to avoid oxidation and ignition. Therefore, a nitrogen gas at a flow rate of 100 ml/min for 1 h was used as the inert carrier gas. Mangrove fibers were labeled as UNM for untreated fiber and TM120, TM140, TM160 and TM180 for mangroves treated at 120 °C, 140 °C, 160 °C and 180 °C, respectively.

Preparation of mangrove fiber/HDPE composite

Composites of untreated and treated were prepared based on the optimal treatment temperature (120 °C) of MF. The pre-mixed portions of MF/HDPE were blended in a twin-screw laboratory compounder (model Brabender KETSE 20/40, Germany) with each screw having a diameter of 20 mm and a *L*:*D* (length to diameter ratio) of 40. The compounding was done at a screw speed of 80 rpm, while the temperatures of the six heating zones were set at 150, 155, 160, 165, 170 and 175 °C. These heating zones produced the actual melt temperature of between 181 and 184 °C. The long strands of extruded composites leaving the circular die of 3 mm were pelletized after cooling in a laboratory pelletizer into a length of about 6 mm. Untreated and treated composites were prepared at 10 wt%, 20 wt% and 30 wt% of MF. Drying of the pelletized extrudates was done in a vacuum oven at 80 °C for about 24 h before being injection molded into dumbbell-shaped tensile test specimens in conformance with ASTM D 638 standard. The model of the injection molding machine was Boy 55 M, Germany, a 55-tonne clamping force injection molding machine in which the mold used for preparing tensile tests specimens was single gated with four cavities. The processing temperature was set between 160 and 190 °C, and the mold temperature was set at 20 °C. The screw speed was maintained at between 30 and 50 rpm at injection pressure of 100–120 bar and cooling time of 120 s.

Characterization of mangrove fiber

Chemical composition

The chemical composition was determined by chemical analysis using the method described by Van Soest [19, 20].

Chemical structure

The chemical structure of untreated and treated samples were recorded using the Perkin-Elmer 400 (USA) Fourier transform infrared spectra (FTIR) spectrometer within 4000–650 cm^{-1} (wavenumber range) at a resolution of 4 cm^{-1} and a total scan of 16.

Color spectroscopy

Colors of mangrove fiber were determined using the CIELAB procedure with a three-axis system: lightness (L^*) = 0% (black) to 100% (white), a^* = green ($-a$) to red ($+a$), b^* = blue ($-b$) to yellow ($+b$). The colors were quantified using an optical spectroscopy instrument (model AvaSoft© 8.5.0-2016 Avantes), Netherland. For any measured color of lightness (L^*), the coordinates (a^*, b^*) locate the color on a rectangular coordinate grid perpendicular to the L^* axis. On the horizontal axis, $+a^*$ indicates a hue of red–purple; $-a^*$, bluish-green. On the vertical axis, $+b^*$ indicates yellow and $-b^*$, blue. Six samples of each of the untreated and treated mangrove fibers were measured, and the average of four reproducible measurements was presented.

Crystalline structure

The crystallinity of mangrove fibers pre- and post-heat treatment was measured by X-ray diffraction (XRD). The sample of the mangrove fiber was set on the sample compartment and flattened to obtain total and unvarying exposure. Samples were analyzed using an Empyrean diffractometer (PANalytical, Netherlands). The analysis was carried out at room temperature with a monochromatic CuKα1 radiation source ($\lambda = 0.154060$ nm) in the step-scan mode at 40 kV, 40 mA with 2θ angle ranging from 10° to 50° with a step size of 0.02° and scanning time of 5 min. Percentage of crystallinity was evaluated to characterize samples' crystallinity (using the Highscoreplus software).

Surface morphology

Hitachi field emission scanning electron microscopy (FESEM) model SU8220 (Japan) was used to examine the surface morphology of the mangrove fibers and the fracture surfaces of the tensile test specimens. The effect of the heat treatment at differing temperatures was investigated using a comparison of the untreated and treated samples. Thin layer of platinum was applied unto MF and fractured surfaces with the aid of a vacuum sputter applicator in order to enhance the quality of the SEM images.

Thermogravimetry analysis (TGA)

The thermogravimetry analyses of the untreated and treated samples were measured using a Perkin-Elmer TGA 6 (USA) in a ceramic crucible. About 6–12 mg was the

amount of sample used for each measurement. All measurements were evaluated by subjecting the sample to heating, from a temperature of 50 °C to 900 °C at a heating scan rate of 20 °C/min under a pure nitrogen environment at a gas flow rate of 20 ml/min.

Characterization of MF/HDPE composites

Tensile properties

Tensile experiments were carried out in line with ASTM D 638 standard [21]. A universal tensile testing machine, modeled Instron 5567, USA, was used with an attached 10 kN load cell and a mechanical extensometer at 5 mm/min (unvarying cross-head speed) at 25 °C. The tensile modulus was calculated at 0.5% strain. At least, ten samples were evaluated for each test. The presented results were taken from the mean of a minimum of six reproducible data.

Flexural properties

This test was carried out with the tensile instrument on a three-point bending mode in accordance with ASTM D 790 standard [22]. Using a span of 50 mm, the injection molded dumbbell-shaped specimens were measured with a maximum deflection of 30 mm and a cross-head speed of 1.31 mm/min. Equation (1) was used to calculate the speed of the cross-head.

$$ZL^2/6d \tag{1}$$

where L specimen's support span, d specimen's depth/thickness and Z is the straining rate of the outer fiber (equal to 0.01). L was fixed at 50 mm. Ten samples were examined. The presented results were generated from the mean of a minimum of six reproducible data.

Results and discussion

Characterization of MF

Chemical composition

The chemical constituents of the (MF) are presented in Table 1. The main compositions of mangrove fibers are cellulose, hemicellulose, lignin, inorganic content (ash) and others. Other constituents of this fiber include very small quantity of starch, free sugars, proteins, holocelluloses, several mineral salts and extractives such as waxes, fatty alcohols and different esters [23, 24]. As illustrated in Table 1, the highest cellulose content of ≈ 56 wt% was obtained at TM120 while UNM contains 46.19 wt% of cellulose. Furthermore, the cellulose contents decrease during subsequent heat

Table 1 Chemical composition of mangrove fibers

Mangrove fiber	Cellulose (wt%)	Hemicellulose (wt%)	Lignin (wt%)	Ash (wt%)	Others (wt%)
UNM	46.19	21.12	30.18	0.95	1.56
TM120	56.21	21.83	20.17	0.95	0.84
TM140	53.93	22.73	20.88	1.04	1.42
TM160	50.50	22.21	21.91	1.04	4.34
TM180	48.06	13.54	27.21	1.13	10.06

modification. As it can be observed in Table 1, the hemicellulose contents of the mangrove fiber are slightly increased to about 21.8 wt% in TM120 compared with UNM. On the other hand, hemicellulose content was drastically reduced to about 14 wt% at TM180. This reduction shows the lack of crystalline nature of hemicelluloses and their sensitivity to dehydration at high temperature [13] However, 30 wt% of lignin content in the untreated fiber was reduced to $\approx$20 wt% at 120 °C but slightly increased upon further heat treatment to 27.21 wt% at TM180. It could be observed that at high temperature, the amount of lignin increased while the amount of carbohydrates decreased. The increase in lignin content does not connote the formation of lignin during the heating process but the reduction in other wood components as suggested by Kamdem et al. [25] Also, some of the thermal degradation products of carbohydrates may be retained in the lignin fraction [13].

Chemical structure

FTIR was carried out on samples of mangrove fibers in order to examine any change in the chemical structure as a result of the thermal modification. Figure 1 shows the typical infrared spectra of mangrove fiber treated at different temperatures. All samples presented similar spectra at two main absorbance peaks, both at higher (wavenumber range 3500–2900 cm^{-1}) and lower (wavenumber range 1700–900 cm^{-1}) regions of wavenumbers. There is a noticeable decrease in the intensity of the absorbance peaks after treatments which indicate chemical structure's transformation of the fiber. At the specific peak of 3343 cm^{-1}, there is reduction in the intensity of absorption peaks from UNM through TM180. The specific peaks at 3343 cm^{-1} and 2902 cm^{-1} are equivalent to OH absorption and prominent CH stretching absorptions, respectively, in cellulose and lignin. The intermolecular H bonds involving C6 positions (primary OH group) in lignin result in the formation of crystalline regions and contribute to the OH bond at 3419/3351 cm^{-1} [26]. The band sighted at 1732 cm^{-1} is a characteristic of C=O stretching of acetyl as well as ester groups of hemicellulose or the ester linkage of carboxylic acid groups in the *p*-coumeric components of lignin, while the decrease in the carbonyl band at 1732 cm^{-1} indicated hemicellulose degradation [14, 27]. The band at 1594 cm^{-1} is attributed to C=C aromatic stretching or bending vibration of lignin. The diminution of the water IR absorption band at 1640 cm^{-1} compared to the C=C skeletal vibration band at 1594 cm^{-1} indicates the drying phase [28]. The band 1504 cm^{-1}

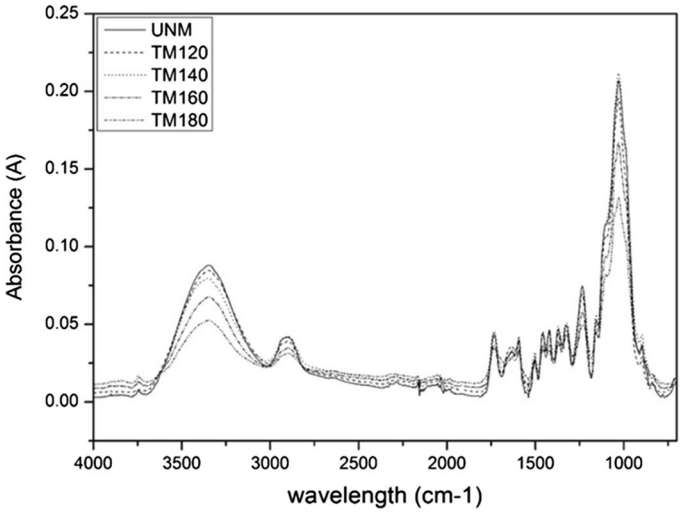

Fig. 1 FTIR absorbance peaks of untreated and treated mangrove fibers

that could be seen in all spectra is ascribed to the aromatic C=C stretching from the aromatic ring of lignin [29]. The peaks at 1315 cm^{-1}, 1225 cm^{-1} and 1027 cm^{-1} are ascribed to amorphous cellulose II, C–O–C aryl alkyl ether of cellulose/lignin and aromatic C-O stretching in cellulose I/cellulose II, respectively [30, 31].

Color spectroscopy

Color spectroscopy is aimed at measuring the impact of thermal treatment on the chemical constituents of MF, irrespective of the color impression of the individual observer by means of objective numbers. Figure 2 shows the average color studies of untreated and treated mangrove fibers as quantified by the CIELAB method. In MF, there is a noticeable increase in the CIE lightness color coordinate at TM120 ($L^* = \approx 56\%$) from $\approx 49\%$ in UNM. L^* decreased with increased process severity which is $\approx 54\%$, 41% and 35% in TM140, TM160 and TM180, respectively. The L^* values of TM120 and TM140 are higher than the untreated which indicate that the colors of these treated samples are slightly lighter than UNM fiber. The results show that the reflectance difference of mangrove fiber after heat treatment is larger than that of untreated. These color differences are due to the extraction of un-cellulosic materials such as lignin, hemicellulose, pectin, wax and other impurities after treatment. Thus, the light cellulosic color is an advantage to the mechanical properties of fiber composite, as the crystalline cellulose, which will impart strength to the composite system is being exposed to the surface of MF fiber [32]. This is expected to enhance better compatibility between the MF and the matrix, thereby improving the stress transfer efficiency of the MF fiber, resulting in improved mechanical property. However, the L^* values of TM160 and TM180 are lower than UNM which indicate darker coloration of the fibers at these treatment temperatures. The darker shades are

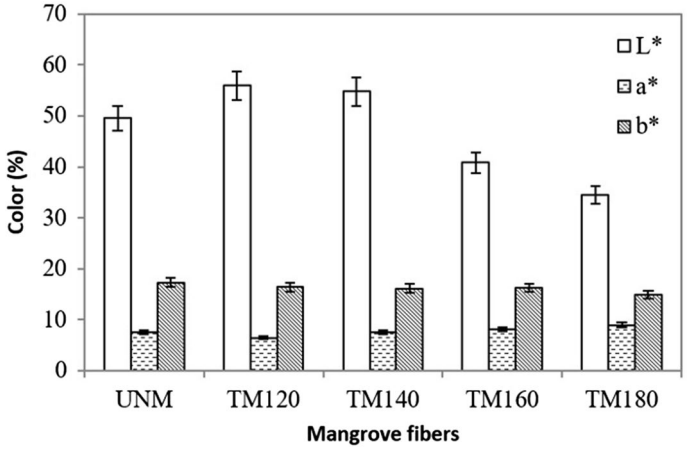

Fig. 2 Color coordinates of mangrove fibers at different modifying temperatures

due to the existence of colored degradation materials that were formed from hemicelluloses and extractives; these probably participate in the formation of color in thermally modified wood. These same conditions were also reported in the previous literature [33]. On the other hand, TM180 showed the highest value of a^* (8.9%) because of the presence of high extractives contents compared to other fibers. Therefore, extractives are important factors determining changes in a^*. The b^* values of 17.29%, 16.38%, 16.14%, 16.21% and 14.95% were obtained in UNM, TM120, TM140, TM160 and TM180, respectively. According to Liu [34], the changes in b^* are related to changes in lignin content during heat treatment.

Surface morphology

Figure 3 shows the scanning electron microscopy (SEM) micrographs of mangrove fibers. The surface morphology of UNM appears smooth due to the presence of foreign materials (impurities) on the fiber surface. However, the treated fibers have rough surfaces which are a likely indication of the partial removal of the outer non-cellulosic layers; these outermost layers are composed of materials such as hemicelluloses, lignin, pectin, wax and other impurities [14]. From the SEM micrograph, TM120 showed evidence of open fissures that will probably enable considerable interlocking of the required matrix during polymer composite production. The surface appearance of TM140 is corrugated, which may not provide adequate interfacial adhesion during fiber composite production. Also, TM160 has rough surfaces without any evidence of opened fissures to allow adequate adhesion between the fiber and the intended polymer matrix; TM180 has rougher, closed and degraded surface.

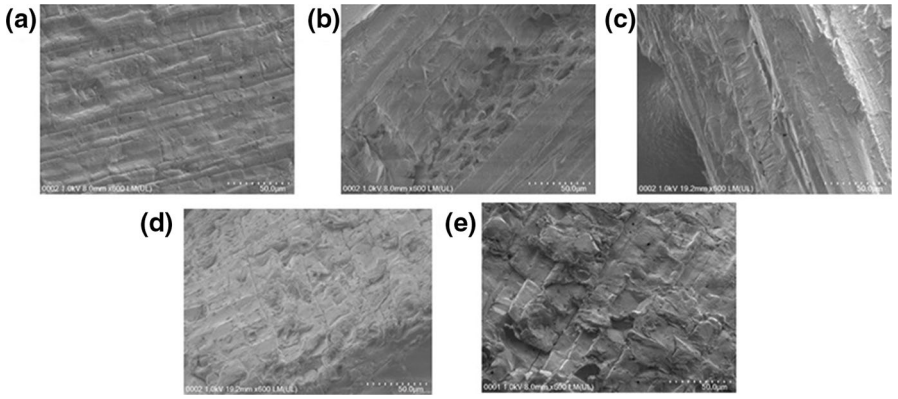

Fig. 3 SEM micrographs of **a** UNM, **b** TM120, **c** TM140, **d** TM160 and **e** TM180

Crystalline structure

The crystalline structures of mangrove fibers were analyzed by X-ray diffraction as shown in Fig. 4. The XRD patterns of these mangrove fibers are elucidated by two characteristic peaks, which were observed at the 2θ position of the XRD diffractogram, the first peak was noted at about 17° and the second strong peak was at about 24°. The similar characteristic peaks of the cellulose at about 24° appear in all samples. According to Thambiraj and Shankaran [35], the peak around 24° is attributed

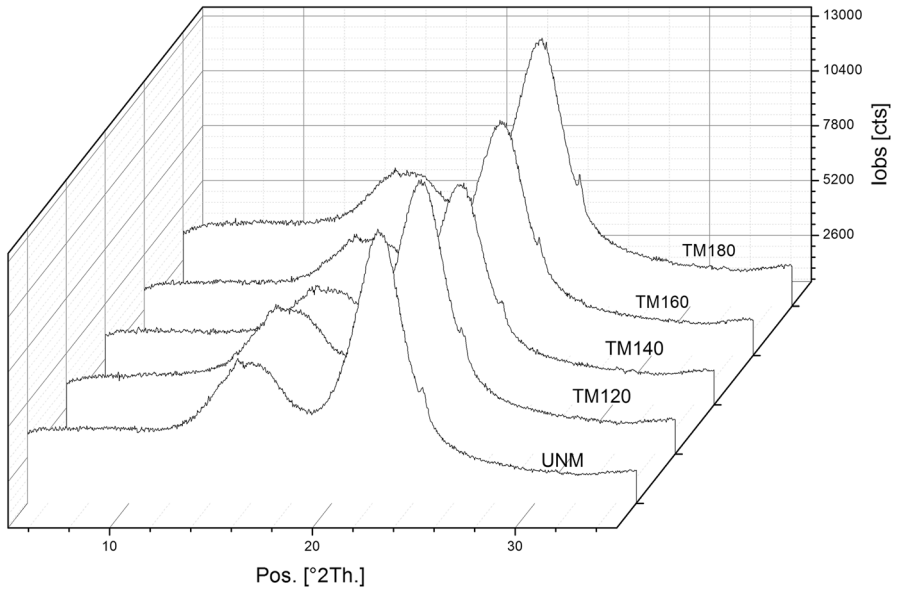

Fig. 4 X-ray diffractogram of mangrove fibers

Table 2 Crystallinity index (CrI) of mangrove fibers

Mangrove fiber	CrI (%)
UNM	49.52
TM120	50.67
TM140	51.77
TM160	56.03
TM180	61.08

Table 3 TGA data of mangrove fibers

Mangrove fiber	T_{onset} (°C)	$T_{50\%}$	T_p (°C)
UNM	269.07	371.46	371.41
TM120	277.28	372.35	374.65
TM140	266.59	369.45	370.38
TM160	250.34	372.58	372.46
TM180	299.90	383.05	375.61

to the typical lattice structure of cellulose indicating the characterization pattern of the amorphous phase. However, the intensities of the peaks at 24° increased with temperature increase, an evidence of changes in wood crystallinity [36] with insignificant differences in the peak intensities of UNM, TM120 and TM140. A less defined peak of about 17° appears in all spectra of the mangrove fiber before and after treatment confirming the results from the contribution of amorphous cellulose and other amorphous components (mainly lignin and hemicellulose) as reported by Maache et al. [2]. Table 2 illustrates the crystallinity indices of mangrove fibers treated at varying temperatures. In this study, the cellulose crystallinity increased as temperature increased. The crystallinity index of UNM is ≈ 49%, which increased to ≈ 51% in TM120 to ≈ 61% in TM180. Generally, the amorphous parts of cellulose are hydrolyzed first, leaving a residue of cellulose with increased degree of crystallinity [25]. As a result of heat modifications, it is observed that hemicelluloses and less ordered cellulose of the mangrove fiber deteriorate, and as a result, the degree of cellulose crystallinity increased. It was suggested by Pereira et al. [33] that amorphous cellulose and some hemicellulose are changed to crystalline structures. Also, the high amount of crystallinity could be as a result of crystallization of amorphous portions due to the re-arrangement/re-orientation of molecules of cellulose within these portions [37].

Thermal stability

The TGA characterization data of mangrove fibers are shown in Table 3 while the thermogravimetric analysis (TGA) and derivative thermogravimetric (DTG) analysis curves are illustrated in Fig. 5a, b, respectively. In TGA, two stages of decomposition are seen, the first stage of decomposition occurred at the region of about 150 °C due to the loss of moisture from the mangrove fiber by evaporation. The

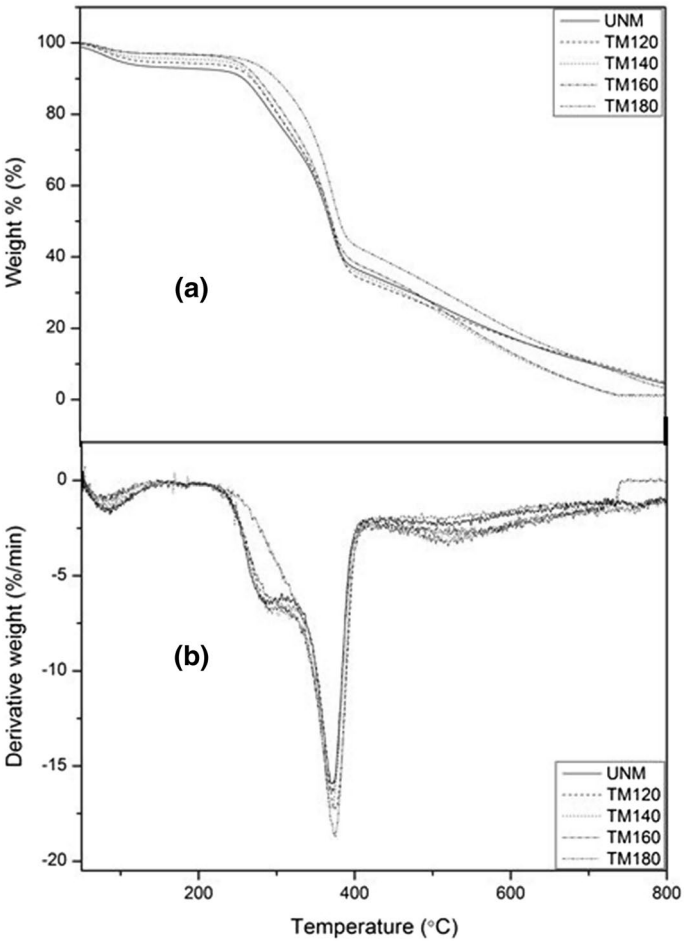

Fig. 5 **a** TGA and **b** DTG thermograms of untreated and treated mangrove particles as a function of modification temperature

second stage occurred at the range between 257 and 390 °C, this is attributed to the decomposition of hemicellulose, cellulose and lignin. Generally, hemicellulose decomposes at 150–350 °C, cellulose decomposes between 240 and 350 °C, and lignin decomposes between 250 and 500 °C [38].

From the TGA curves, the onsets of degradation (T_{onset}) of mangrove fibers are observed at temperatures of about 269–300 °C, an indication of hemicellulose degradation and the onset of cellulose decomposition. The T_{onset} of UNM is ≈ 270 °C and shifted to a higher temperature at TM120, TM140, TM160 and TM180 to ≈ 277 °C, 267 °C, 250 °C and 300 °C, respectively. Consequently, the 50% mass loss of UNM, TM120, TM140, TM160 and TM180 occurred at temperatures of about 371 °C, 372 °C, 369 °C, 372.6 °C and 383 °C, respectively. The maximum degradation temperature (T_p) is a temperature that illustrates the highest mass loss which represents

the peak point in the derivative curves. In order to have a comprehensive view of mass loss caused by temperatures, the derivative curves obtained by the calculation of deriving weight loss against temperature data are given in Fig. 5b and Table 3. Mangrove fiber being a chemically active lignocellulose material decomposed in the range of 150–400 °C. The highest mass loss (main peak) of mangrove fiber occurred at temperatures between 370 and 376 °C. The T_p of UNM, TM120, TM140, TM160 and TM180 are about 371 °C, 375 °C, 370 °C, 372 °C and 376 °C. Hence, it can be deduced that mangrove fibers are thermally stable with TM120 and TM180 showing the highest resistance to heat degradation. This is also an evidence of the high content of lignin observed in the chemical content of mangrove fiber (Table 1).

Characterization of MF/HDPE composites

Tensile properties

Figure 6 depicts the influence of MF content on the tensile strength of MF/HDPE composites. The ratio of the force required to break a sample to its cross-sectional area is referred to as the tensile strength of a material. It represents the maximum load that a material can hold while still performing its designated role. The results obtained show that heat treatment had positive influence on MF/HDPE composites to a certain extent. The values of the σ are 19.13, 18.20 and 18.14 MPa for 10, 20 and 30% by weight of untreated composites, respectively. Meanwhile, the treated composites recorded higher values of 20.39, 20.26 and 18.80 MPa at 10, 20 and

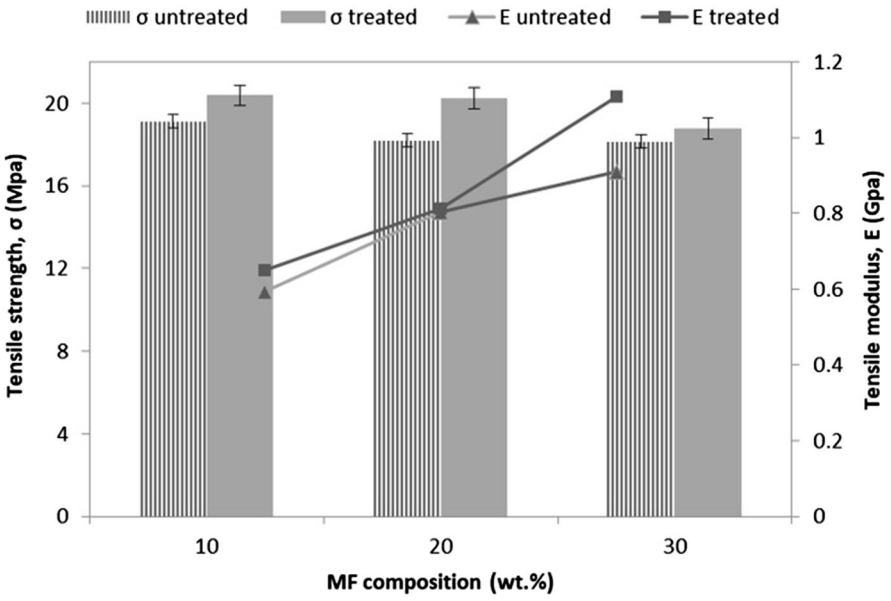

Fig. 6 Tensile strength and tensile modulus of untreated and treated MF/HDPE composites

30% by weight of treated composites, respectively. These results are also buttressed by SEM images Fig. 7a, b. The images of the untreated composites reveal irregular fractured surfaces with clean and uncoated fibers as a result of the incompatibility of the fiber and HDPE matrix. On the other hand, fiber pullouts are not so prominent in treated composites compared to the untreated composites and the fibers are seen to be attached to and embedded within the matrix. These show evidences of enhanced wetting of the heat-treated MF by the HDPE matrix. These observations are the reason for the higher tensile strength and modulus obtained for heat-treated mangrove composites [38]. Nevertheless, the σ of both untreated and treated composites decreased with the increase in weight fraction of fiber content owing to agglomeration of fiber within the matrix as revealed in Fig. 7c, d. This may be due to the inability of the matrix to completely wet wood fibers, leading to an increase in fiber–fiber contact (Fig. 7d), and consequently, premature failure as wood content increases [38]. It could also be likened to the poor fiber-matrix interaction, resulting in poor interfacial interaction as tensile strength depends strongly upon the filler-matrix adhesion at the interface [39, 40]. The percentage decrease obtained for untreated composites is about 7%, 11% and 12%, as against 1%, 2% and 9% obtained for treated composites at 10 wt%, 20 wt% and 30 wt%, respectively, compared to the σ of pure matrix (20.6 MPa). The decrease in maximum tensile stress indicates that fiber particles debonded from the matrix before or at the start of plastic deformation. Due to the debonding, the strain constraint is released; therefore, tensile yield stress is reduced [41].

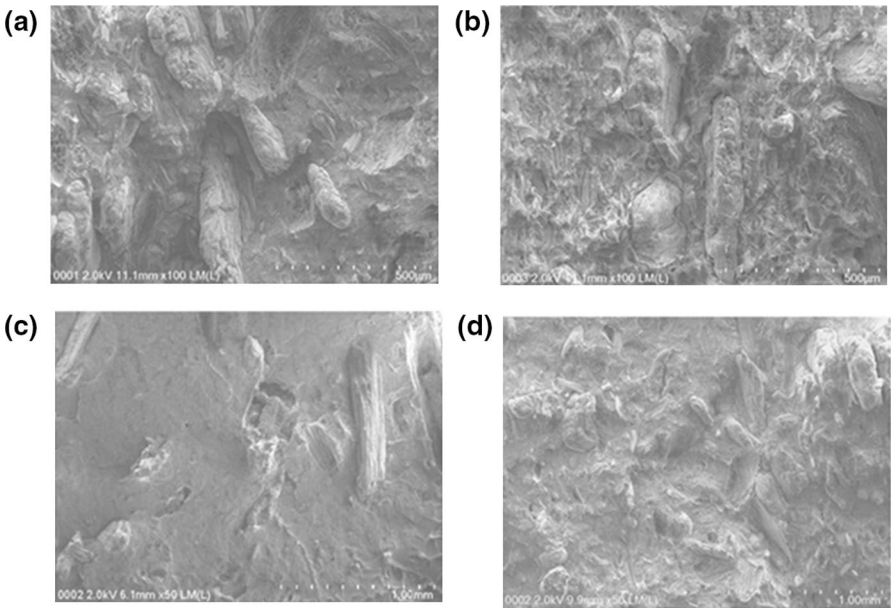

Fig. 7 SEM micrographs of tensile fractured specimen of untreated and treated MF/HDPE composites: **a** 10 wt% untreated, **b** 10 wt% treated, **c** 30 wt% untreated and **d** 30 wt% treated MF/HDPE

The secondary axis of Fig. 6 depicts the tensile modulus of untreated and heat-treated MF/HDPE composites. Tensile modulus data are used to measure the resistance of a material to deformation during the application of external forces. It is effectively a measure of the stiffness of a material. Generally, tensile modulus increases with the increase in wood contents. Therefore, composites of higher fiber loading are able to withstand more force/load. An increasing trend of E was noted in untreated composites at all fiber loadings, with percentage increase of 29%, 74% and 97% for samples containing 10%, 20% and 30% by weight of MF, respectively, compared to the neat HDPE matrix (0.462 GPa). An increase in modulus of treated composites relative to the untreated indicates better adhesion/wetting of the fiber by the matrix. A percentage increase of 40% at 10 wt%, 76% at 20 wt% and 140% at 30 wt% is obtained for heat-treated composites relative to the neat HDPE due to enhanced interaction between the MF and HDPE matrix.

The bar chart of tensile strain of the untreated and treated composites is illustrated in Fig. 8. Tensile strain is the strain correlating to the yield point. It is also known as elongation at break. Generally, the inclusion of fiber reduced the tensile strain of the composites. Increasing the amount of filler in composites decreased the amount of polymer available for elongation and increased the possibility of fiber agglomeration [39]. In the case of MF/HDPE composites, the ε of untreated composites is higher than the treated. The values obtained for the ε of both untreated and treated composites are $\approx$14.5%, 10.3%, 7.4% and 14%, 9.9%, 7.2% for 10 wt%, 20 wt% and 30 wt%, respectively. These observations show little significant difference in the ε of both composites.

Flexural characteristics

A material's resistance to bend is known as the flexural characteristics. Flexural strength increases with the increase in filler loading. The introduction of wood fibers renders the flexible HDPE matrix inflexible; hence, flexural strength is increased. As shown in Fig. 9, the flexural strength of both untreated and treated composites increased as fiber content increased. Treated composites show higher flexural strength with an increasing trend of about 8%, 29% and 42% at all filler loadings of

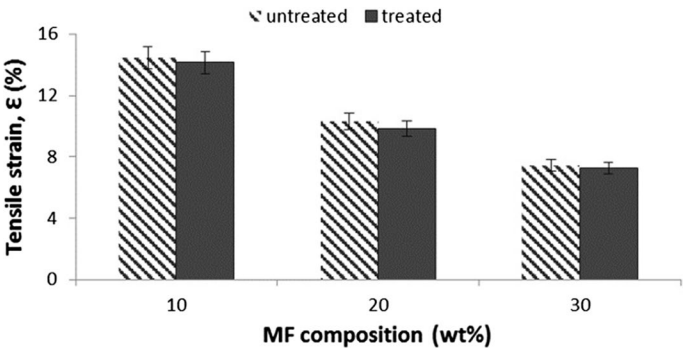

Fig. 8 Tensile strains of untreated and treated MF/HDPE composites

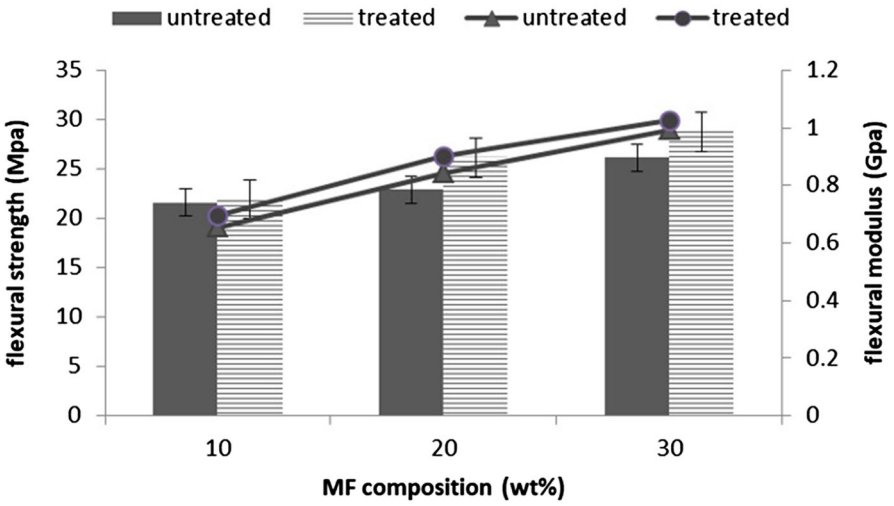

Fig. 9 Flexural strength and flexural modulus of untreated and treated MF/HDPE composites

10%, 20% and 30% by weight, respectively, relative to the pure HDPE (20.219 MPa). Meanwhile, the untreated composites exhibit about 7%, 13% and 29% increase in 10 wt%, 20 wt% and 30 wt%, respectively, when compared to the pure HDPE. These observations may be due to the reinforcing effects of MP on HDPE which led to an increase in the transfer of stress from the fibers to the matrix [38] as well as possible enhanced adhesion on the part of the treated composites. The flexural moduli of untreated and treated composites are also shown on the secondary axis in Fig. 9. These results show the same trend as flexural strength.

Flexural displacement reduces as the filler content increases. This is due to the fact that natural fibers exhibit less strain at break than the matrix. Hence, the addition of natural fillers renders the matrix more rigid by decreasing the flexibility of the polymer chain, thereby leading to reduced flexural displacement. Figure 10 shows the flexural

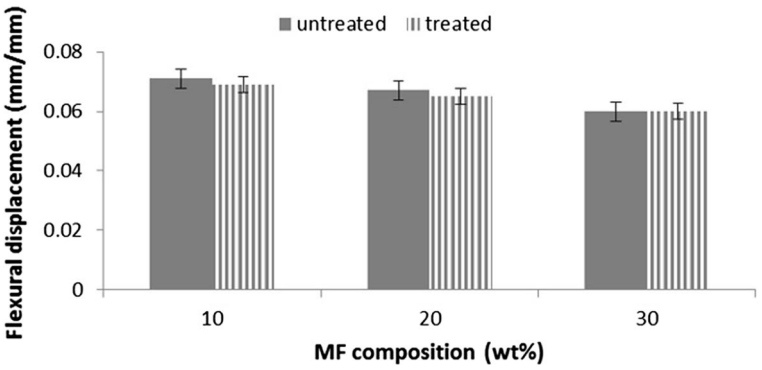

Fig. 10 Flexural displacement of untreated and treated MF/HDPE composites

displacement of untreated and treated composites. The displacement of pure HDPE, 10%, 20% and 30%, by weight of untreated composites is 0.073, 0.071, 0.067 and 0.06 GPa, respectively. Meanwhile, those of the treated composites were found to be 0.069, 0.065 and 0.06 GPa as fiber loading increased. These show an improved wettability of heat-treated MF by the HDPE, thereby not yielding to bending as the untreated counterparts. However, the same flexural displacement was recorded for both untreated and treated composites at 30 wt%.

Conclusions

The hydrophilicity of mangrove fibers was successfully improved by heat treatment. The results obtained showed the removal of hemicellulose, lignin, pectin, waxy substances and impurities from the outer surface of the mangrove cell wall, thereby indicating an effective heat treatment. The chemical composition of the MF revealed an increased amount of cellulose content at 120 °C. FTIR spectroscopy indicated chemostructural changes, while the highest thermal stability was observed at 120 °C and 180 °C. The crystallinity index and morphological changes occurred at different treatment temperatures. These results showed that these characterizations are important factors in establishing the properties of the fiber.

The tensile modulus of both untreated and treated MF/HDPE composites increased with increase in MF content, while the tensile strength and strain were found to decrease. It is worthy to note that treated composites showed better tensile properties relative to the untreated ones. The flexural strength and modulus of both untreated and treated MF/HDPE composites increased with the increase in MF content, while the flexural displacement reduced. This is as a result of the reinforcing impact of the wood fiber on the matrix. Here, the treated composites exhibited higher flexural strength and flexural modulus than the untreated ones. From the analysis of fractured surfaces, the main causes of failure were identified in MF/HDPE composites. In the untreated composites, debonding, fiber pullouts and non-uniform distribution of fibers in the matrix were prominent, whereas fibers delamination and fibers attachment to the matrix were seen in the treated composites, thus indicating an enhanced interfacial adhesion.

Acknowledgements This study was supported by University of Malaya, Kuala Lumpur, Malaysia, through IPPP research Grant No. PG137-2016A.

Compliance with Ethical Standards

Conflict of interest On behalf of all authors, the corresponding author states that there is no conflict of interest.

References

1. Ali A, Shaker K, Nawab Y, Jabbar M, Hussain T, Militky J, Baheti V (2016) Hydrophobic treatment of natural fibers and their composites—a review. J Ind Text. https://doi.org/10.1177/1528083716654468

2. Maache M, Bezazi A, Amroune S, Scarpa F, Dufresne A (2017) Characterization of a novel natural cellulosic fiber from *Juncus effusus* L. Carbohyd Polym 171:163–172. https://doi.org/10.1016/j.carbpol.2017.04.096
3. Xiong X, Shen SZ, Hua L, Liu JZ, Li X, Wan X, Miao M (2018) Finite element models of natural fibers and their composites: a review. J Reinf Plast Compos 37(9):617–635. https://doi.org/10.1177/0731684418755552
4. Wang P, Liu J, Yu W, Zhou C (2011) Dynamic rheological properties of wood polymer composites: from linear to nonlinear behaviors. Polym Bull 66(5):683–701. https://doi.org/10.1007/s00289-010-0382-y
5. Nirmal U, Hashim J, Ahmad MM (2015) A review on tribological performance of natural fibre polymeric composites. Tribol Int 83:77–104
6. Nourbakhsh A, Ashori A, Ziaei Tabari H, Rezaei F (2010) Mechanical and thermo-chemical properties of wood-flour/polypropylene blends. Polym Bull 65(7):691–700. https://doi.org/10.1007/s00289-010-0288-8
7. Njuguna J, Wambua P, Pielichowski K, Kayvantash K (2011) Natural fibre-reinforced polymer composites and nanocomposites for automotive applications. In: Kalia S, Kaith SB, Kaur I (eds) Cellulose fibers: bio- and nano-polymer composites: green chemistry and technology. Springer, Berlin, pp 661–700. https://doi.org/10.1007/978-3-642-17370-7_23
8. Siengchin S (2012) Impact, thermal and mechanical properties of high density polyethylene/flax/SiO_2 composites: effect of flax reinforcing structures. J Reinf Plast Compos 31(14):959–966
9. Sinha E, Rout SK (2008) Influence of fibre-surface treatment on structural, thermal and mechanical properties of jute. J Mater Sci 43(8):2590–2601. https://doi.org/10.1007/s10853-008-2478-4
10. Ayrilmis N, Jarusombuti S, Fueangvivat V, Bauchongkol P (2011) Effect of thermal-treatment of wood fibres on properties of flat-pressed wood plastic composites. Polym Degrad Stab 96(5):818–822
11. Boonstra MJ, Van Acker J, Tjeerdsma BF, Kegel EV (2007) Strength properties of thermally modified softwoods and its relation to polymeric structural wood constituents. Ann For Sci 64(7):679–690
12. Fang L, Xiong X, Wang X, Chen H, Mo X (2017) Effects of surface modification methods on mechanical and interfacial properties of high-density polyethylene-bonded wood veneer composites. J Wood Sci 63(1):65–73
13. Yildiz S, Gezer ED, Yildiz UC (2006) Mechanical and chemical behavior of spruce wood modified by heat. Build Environ 41(12):1762–1766
14. dos Santos RM, Neto WPF, Silvério HA, Martins DF, Dantas NO, Pasquini D (2013) Cellulose nanocrystals from pineapple leaf, a new approach for the reuse of this agro-waste. Ind Crops Prod 50:707–714
15. Joel EL, Bhimba V (2010) Isolation and characterization of secondary metabolites from the mangrove plant *Rhizophora mucronata*. Asian Pac J Trop Med 3(8):602–604
16. Bandaranayake WM (1998) Traditional and medicinal uses of mangroves. Mangroves Salt Marshes 2(3):133–148. https://doi.org/10.1023/a:1009988607044
17. Liang J-Z, Yang Q-Q (2007) Mechanical, thermal, and flow properties of HDPE-mica composites. J Thermoplast Compos Mater 20(2):225–236
18. Bouafif H, Koubaa A, Perré P, Cloutier A (2009) Effects of fiber characteristics on the physical and mechanical properties of wood plastic composites. Compos A Appl Sci Manuf 40(12):1975–1981
19. Van Soest P, Robertson J (1979) Systems of analysis for evaluating fibrous feeds. In: Standardization of analytical methodology for feeds: proceedings…. IDRC, Ottawa, ON, Canada
20. Fasanella CC, Montes CR, Rossi ML, Aguiar MM, Ferreira LF, Pupo MM, Salazar-Banda GR, Monteiro R (2018) Microscopic analysis of sugarcane bagasse following chemical and fungal treatment. Cellul Chem Technol 52(1–2):59–64
21. ASTM (2014) ASTM D638 standard test method for tensile properties of plastics. ASTM International, West Conshohocken
22. ASTM (2017) ASTM D790-17 standard test methods for flexural properties of unreinforced and reinforced plastics and electrical insulating materials. ASTM International, West Conshohocken, Pennsylvania
23. Baltazar-y-Jimenez A, Bismarck A (2007) Wetting behaviour, moisture up-take and electrokinetic properties of lignocellulosic fibres. Cellulose 14(2):115–127

24. Baltazar-y-Jimenez A, Bistritz M, Schulz E, Bismarck A (2008) Atmospheric air pressure plasma treatment of lignocellulosic fibres: impact on mechanical properties and adhesion to cellulose acetate butyrate. Compos Sci Technol 68(1):215–227
25. Kamdem D, Pizzi A, Jermannaud A (2002) Durability of heat-treated wood. Eur J Wood Wood Prod 60(1):1–6
26. Sheltami RM, Abdullah I, Ahmad I, Dufresne A, Kargarzadeh H (2012) Extraction of cellulose nanocrystals from mengkuang leaves (*Pandanus tectorius*). Carbohyd Polym 88(2):772–779
27. Esteves B, Marques AV, Domingos I, Pereira H (2008) Heat-induced colour changes of pine (*Pinus pinaster*) and eucalypt (*Eucalyptus globulus*) wood. Wood Sci Technol 42(5):369–384
28. Hakkou M, Pétrissans M, Zoulalian A, Gérardin P (2005) Investigation of wood wettability changes during heat treatment on the basis of chemical analysis. Polym Degrad Stab 89(1):1–5. https://doi.org/10.1016/j.polymdegradstab.2004.10.017
29. Ahmadzadeh A, Zakaria S (2008) Preparation of novolak resin by liquefaction of oil palm empty fruit bunches (EFB) and characterization of EFB residue. Polym Plast Technol Eng 48(1):10–16
30. Morán JI, Alvarez VA, Cyras VP, Vázquez A (2008) Extraction of cellulose and preparation of nanocellulose from sisal fibers. Cellulose 15(1):149–159
31. Baharuddin AS, Sulaiman A, Kim DH, Mokhtar MN, Hassan MA, Wakisaka M, Shirai Y, Nishida H (2013) Selective component degradation of oil palm empty fruit bunches (OPEFB) using high-pressure steam. Biomass Bioenergy 55:268–275
32. Mariano M, El Kissi N, Dufresne A (2014) Cellulose nanocrystals and related nanocomposites: review of some properties and challenges. J Polym Sci, Part B: Polym Phys 52(12):791–806
33. Pereira H, Graça J, Rodrigues J (2003) Wood chemistry in relation to quality. In: Barnett J, Jeronimidis G (eds) Wood quality and its biological basis, Wiley, pp 53–86
34. Liu R, Pang X, Yang Z (2017) Measurement of three wood materials against weathering during long natural sunlight exposure. Measurement 102:179–185
35. Thambiraj S, Shankaran DR (2017) Preparation and physicochemical characterization of cellulose nanocrystals from industrial waste cotton. Appl Surf Sci 412:405–416
36. Aydemir D, Kiziltas A, Erbas Kiziltas E, Gardner DJ, Gunduz G (2015) Heat treated wood–nylon 6 composites. Compos B Eng 68:414–423. https://doi.org/10.1016/j.compositesb.2014.08.040
37. Abdullah M, Nazir M, Raza M, Wahjoedi B, Yussof A (2016) Autoclave and ultra-sonication treatments of oil palm empty fruit bunch fibers for cellulose extraction and its polypropylene composite properties. J Clean Prod 126:686–697
38. Lafia-Araga RA, Hassan A, Yahya R, Rahman NA, Hornsby PR, Heidarian J (2012) Thermal and mechanical properties of treated and untreated Red Balau (*Shorea dipterocarpaceae*)/LDPE composites. J Reinf Plast Compos 31(4):215–224
39. Salleh FM, Hassan A, Yahya R, Azzahari AD (2014) Effects of extrusion temperature on the rheological, dynamic mechanical and tensile properties of kenaf fiber/HDPE composites. Compos B Eng 58:259–266
40. Petchwattana N, Covavisaruch S, Chanakul S (2012) Mechanical properties, thermal degradation and natural weathering of high density polyethylene/rice hull composites compatibilized with maleic anhydride grafted polyethylene. J Polym Res 19(7):9921
41. Pérez E, Famá L, Pardo S, Abad M, Bernal C (2012) Tensile and fracture behaviour of PP/wood flour composites. Compos B Eng 43(7):2795–2800

Publisher's Note Springer Nature remains neutral with regard to jurisdictional claims in published maps and institutional affiliations.

Affiliations

Ganiyat Olusola Adebayo[1,2] · Aziz Hassan[1] · Rosiyah Yahya[1] · Normasmira Abd Rahman[1] · Ruth Lafia-Araga[3]

[1] Polymer and Composite Materials Research Laboratory, Department of Chemistry, Faculty of Science, University of Malaya, 50603 Kuala Lumpur, Malaysia

[2] Standards Organisation of Nigeria, Operational Headquarters, Lekki Peninsula Scheme 1, 101233 Lekki, Lagos, Nigeria

[3] Department of Chemistry, School of Physical Sciences, Federal University of Technology, Minna, Niger State, Nigeria